Afyon Kocatepe Üniversitesi Fen ve Mühendislik Bilimleri Dergisi
Afyon Kocatepe University – Journal of Science and Engineering
https://dergipark.org.tr/tr/pub/akufemubid

Araştırma Makalesi / Research Article
DOI: https://doi.org/10.35414/akufemubid.1411091
AKÜ FEMÜBİD **24** (2024) 041102 (789-797)
AKU J. Sci. Eng. **24** (2024) 041102 (789-797)

A Study on the Effect of Addition Li, Na, and K on the Radiation Shielding Capabilities of B_2O_3-TeO_2-ZnO-PbF_2-Er_2O_3 Glass Structure

Makale Bilgisi / Article Info
Alındı/Received: 28.12.2023
Kabul/Accepted: 20.06.2024
Yayımlandı/Published: 20.08.2024

Li, Na ve K İlavesinin B_2O_3-TeO_2-ZnO-PbF_2-Er_2O_3 Cam Yapısının Radyasyondan Korunma Yetenekleri Üzerindeki Etkisinin Değerlendirilmesi

Hatice YILMAZ ALAN *

Institute of Nuclear Sciences, Ankara University, 06830, Ankara, Turkey.

Abstract

The radiation shielding qualities of the B_2O_3-TeO_2-ZnO-PbF_2_M_2O/MF (M= Li, Na, and K) glass samples doped with Er_2O_3 were investigated in this research. The Phy-X/PSD software was simulated to evaluate the attenuation factors of glass systems at various energy regions. The results show that the addition of LiF instead of Li_2O, Na_2O, K_2O, NaF, or KF to the base glass system (B_2O_3-TeO_2-ZnO-PbF_2-Er_2O_3) leads to an increase in the density of the glass and an increase in the linear attenuation coefficient. Also, it is seen that for the E4 sample (B_2O_3-TeO_2-ZnO-PbF_2-Er_2O_3-LiF), a decrease in half value layers and tenth value layers in high energy region 10-15 MeV.

Anahtar Kelimeler: *Glass; Phy-X/PSD; Gamma Radiation; Shielding Parameters.*

Öz

Bu çalışmada, Er_2O_3 katkılı B_2O_3-TeO_2-ZnO-PbF_2_M_2O/MF (M=Li, Na ve K) cam örneklerinin radyasyondan korunma kabiliyetleri araştırıldı. Cam sistemlerinin çeşitli enerji bölgelerindeki radyasyon-zayıflatma faktörlerini değerlendirmek için Phy-X/PSD yazılımı kullanıldı. Sonuçlar, temel cam sisteminde (B_2O_3-TeO_2-ZnO-PbF_2-Er_2O_3), Li_2O, Na_2O, K_2O, NaF veya KF yerine LiF eklenmesinin ana cam yoğunluğunda bir artışa ve lineer zayıflatma katsayısı değerlerinde bir artışa yol açtığını göstermektedir. Ayrıca E4 numunesi (B_2O_3-TeO_2-ZnO-PbF_2-Er_2O_3-LiF) için yüksek enerji bölgesinde yani 10-15 MeV enerjilerde yarı değer katmanı kalınlığı ve ondabir katman kalınlığı değerlerinde azalma olduğu görülmektedir.

Keywords: *Cam; Phy-X/PSD; Gama Radyasyonu; Zırhlama Parametreleri.*

1. Introduction

The radiation technology properly serves diverse fields such as industry, nuclear facilities, and hospitals (for diagnostic and radiotherapy). At this stage, it is very critical to protect the population from the hazardous effects of radiation. For this reason, studies on protection parameters and protection materials in radiation applications are important. The studies on radiation attenuation properties of various compounds, alloys, glasses, polymers, and other materials are a primary goal to determine the potential of the shielding materials. Lead is one of the most known absorber materials used for radiation shields owing to its high density and high atomic number (Mokhtari *et al*. 2021). Lead is a highly toxic and heavy material. Because of this, the lead can give rise to major long-term destruction as a result of not being taken care of carefully. For this reason, research is these days focused on finding effective substitutes. Concretes are widely used for gamma-ray and neutron shielding thanks to their high durability, easily modifiable, structural properties, and very low cost, merely concretes have disadvantages such as non-transparency, high sensitivity to moisture, and immobility. The other material, alloys is also used as shielding materials that form a mixture of elements and metals (Al-Hadeethi and Sayyed 2020a).

In recent years, various studies have been performed to adjust the shielding efficiency of glass compounds against to ionizing radiation. Glasses are another alternative to standard protective materials thanks to their optical, chemical, physical, and thermal properties, and can be easily produced. Glass-based materials are an important type of radiation shield in medical and nuclear fields and many other applications. Adding several kinds of oxide substances can improve the performance of the glass structures against radiation. Nowadays, glasses encapsulating metal oxides such as bismuth or zinc are in

*Sorumlu Yazar/Corresponding Author: Hatice YILMAZ ALAN e-posta/e-mail: hyalan@ankara.edu.tr

prospect as shielding material. Glasses have desirable shielding features such as optical transparency, chemical, mechanical, and structural capabilities, absorption characteristics, thermal stability, manufacturing simplicity, an easily modifiable structure, low melting point, and addition to different materials. Different types of additives can be added to the glasses at different ratios depending on the purpose of the improvement. For example, the addition of barium, bismuth, or tungsten to borate glasses, raises radiation protection capabilities. For instance, doping zinc oxide to the borate glass enhances thermal stability (Yılmaz *et al*. 2023). On the other part, phosphate-based glasses are a critical material because of their typical features such as low melting temperatures, and thermal expansion coefficients (Agar *et al*. 2019, Metwalli *et al*. 2004).

Tellurite-based glasses have good physical properties, such as low phonon energy and low melting temperature, as compared to other glass (Effendy *et al*. 2021). The rigidity and optical characteristics of glass structure should be unaffected by irradiation (Abou Hussein *et al*. 2021). The chemical properties of additive oxide are also important parameters for the glass formation and structure. Boron trioxide has good thermal shock resistance metals (Abou Hussein *et al*. 2021). Additionally, Li_2O can be added to glass samples to increase mechanical stability (Lakshminarayana *et al*. 2017). To obtain higher shielding capacity by increasing the total density glass modifiers add the heavy metals oxides (HMOs) such as Bi_2O_3 and PbO to the glass structure (Almuqrin *et al*. 2021).

Heavy metal oxides (HMOs) are often added to glass compositions to improve the radiation shielding properties of glass structures. HMOs are high-density metal oxides. The HMOs can greatly increase the density of the glass matrix, and that is usually associated with better shielding performance. By force of its high density and high attenuation capabilities, Bi_2O_3 is frequently used as a HMO. Due to radiation shielding properties, Bi_2O_3 is also often used as a substitute for lead. Depending on the compound of the glass matrix, Bi_2O_3 can act as a glass modifier or a glass former. ZnO is also an important compound used to lower melting points (replacing PbO) when forming oxide glass.

Doping heavy elements such as tantalum, barium, lead, bismuth, or tungsten to borate glasses, increases the glass samples' radiation protection capabilities. Besides, adding aluminum oxide or calcium oxide can improve chemical abilities (Sayyed 2023, Susoy 2020, Tekin *et al*. 2019, Yilmaz *et al*. 2023, Zaid *et al*. 2012). Adding heavy metal oxides to the glass system increases the effective atomic number value. On the other part, heavy metal fluoride-based glasses (HMF) have a strong upconversion luminescence thanks to low phonon energy and non-radiative loss infrared transmission (El-Denglawey *et al*. 2021). Development of modern technology and the health sector, radiation applications are becoming more prominent day by day, and radiation protection studies are gaining importance. The effective atomic number (Z_{eff}) is one of the most critical parameters during the radiation interaction with different types material. Besides Z_{eff}, mean free path (MFP), half value layer (HVL), linear attenuation coefficient (LAC), mass attenuation coefficient (MAC), etc. are the other important parameters for the shielding process. In addition to experimental studies, some calculation programs are used to carry out preliminary studies of applications at all times or high doses (Geant4, Fluka, Monte Carlo, etc...). It is also used in different codes such as SRIM, ESTAR, PAGEX, WinXCOM, ZEXTRa, and Phy-X/PSD to calculate radiation attenuation parameters. Sakar et al. (2020) developed a new software that can compute many attenuation parameters named Phy-X/PSD. This software can estimate parameters such as linear attenuation coefficient (LAC), mass attenuation coefficient (MAC), effective conductivity (C_{eff}), electron density (N_{eff}), half-value layer (HVL), tenth value layer (TVL), mean free path (MFP), effective atomic number (Z_{eff}), energy absorption, buildup factors (EABF) and, exposure buildup factors (EBF) and also the fast neutron removal cross-section (FNRCS) (Ozpolat *et al*, 2020, URL 1).

The Phy-X/PSD software can run data in the continuous energy region (1keV-100GeV). The compounds of the selected materials can be identified in Phy-X/PSD software in wt% or mol%. The densities of the materials are entered into the program as input. This Phy-X/PSD software is stored at https://phy-x.net/ (URL1). Singh et al. (2014) utilized the radiation shielding abilities of silicate and borate glass structures including HMOs for neutron and gamma rays. Almuqrin et al. (2021) estimated the gamma ray attenuation and radiation shielding parameters of the Li_2O-K_2O-B_2O_3-PbO glass system. The effect of PbF_2 (lead-fluoride-based) based glasses was studied by El-Denglawey et al. (2021). Katubi et al. (2022) investigated to shielding capabilities of the B_2O_3-Li_2O-Na_2O-ZnO glass system. Karpuz mentioned the changes observed with the addition of different amounts of B_2O_3 in her study. The results showed that as the

weight fraction of boron oxide added to glass structures increased, the shielding ability also increased (Karpuz 2023). Akkurt and Malidarre (2022) calculated the structural, physical, and mechanical capabilities of marble concrete with Phy-X/PSD codes. The shielding performances of the CaF_2-BaO-P_2O_5 glass structure were evaluated using Phy-X/PSD (Hadeethi and Sayyed 2020). Alan et al. (2023) studied on effects of gadolinium and cerium elements on the tellurite glasses system. Radiation shielding parameters of CoCrFeNiTiAlx alloys were calculated by Arpaci and Aygun (2022) with Phy-X/PSD and EpiXS codes. Şengül measured the linear attenuation coefficients of two different polymer biomaterials both with the help of the GAMOS program and experimentally and compared the results with the XCOM database values (Şengül 2023). Yılmaz et al. (2020) examined the structures of erbium oxide and cerium oxide-doped borosilicate glasses. As a result, they reported that Er_2O_3 doped samples in borosilicate glass structures gave better results than CeO_2 doped samples (Yılmaz et al. 2020). The radiation shielding parameters of silicate-based bioactive glass powders containing erbium(III) and terbium(III) were examined by Deliormanli et al. (2021).

The importance of Er_2O_3 contribution in glass structures containing Si/Cd/Li/Gd was investigated by Al-Buriahi et al. (2021). Lakshminarayana et al. (2023) examined the optical, structural, and thermal characteristics of B_2O_3-TeO_2-ZnO-PbF_2_M_2O/MF (M is equal to the Na, K, and Li) glass samples doped with Er. The radiation shielding abilities of Ni-based alloys were examined by Aygun and Aygun (2023). Khattari and Al-Buriahi (2022) were studied on barium zinc aluminoborosilicate. ALMisned et al. (2023) studied boron oxide and bismuth oxide substitution in bismuth-boro-zinc glasses. Rammah et al examined the ZnO doping on TeO_2-Li_2O-ZnO glass structures using MCNP5 simulations. They emphasized that the addition of ZnO improved the shielding properties and that samples containing high concentration ZnO decreased the ten value layer and mean free path parameters as gamma shielding parameters and increased the linear attenuation coefficient parameter (Rammah *et al*. 2020). The mechanical features and shielding abilities of TeO_2-PbF_2 glasses were calculated by Rammah et al. (2021). Oruncak discussed the shielding properties of glass structures formed by doping selenium, tellurium, and silver in different proportions. It was reported that adding Ag increased glasses shielding ability (Oruncak 2023). Malidarre et al have discussed the shielding abilities of fast neutrons by doping hydroxyapatite and Fe_2O_3 (iron oxide) composites. They found that as the Fe_2O_3 ratio increased, fast neutron removal cross section values also increased. Because adding Fe_2O_3 increased the density (Malidarre *et al*. 2021).

In this study, six (E1-E6) different glass samples were studied as synthesized in the cited research (Lakshminarayana *et al*, 2023). The densities of E1, E2, E3, E4, E5, and E6 glass samples were 3.513 g/cm^3, 3.560 g/cm^3, 3.576 g/cm^3, 3.643 g/cm^3, 3.598 g/cm^3, and 3.559 g/cm^3 (Lakshminarayana *et al*, 2023).

2. Materyal ve Metot / Materials and Methods

2.1 2.1 The Phy-X/PSD online software

The Phy-X/PSD online software was used for the calculation of the attenuation parameters of six different glass samples in this study. Firstly, the composition of the material to be used in the estimating must be defined. The material compositions can be entered into the program such as weight or mole fraction. The user must ensure that the sum of the molar or weight fractions equals 100 or 1, and, where appropriate, the user must normalize them before inputting them into the software. There is no limit to adding compounds or elements in the software. Two energy ranges are pre-defined in the software as 15keV-15MeV and 1keV-100GeV (URL 1). This software is stored at https://phy-x.net/ (URL 1) and the user must access this web page for the use of this calculation code.

2.2 Theoretical background

When the material is positioned in the way of gamma-ray or X-ray, the beam's intensity attenuates according to Beer Lambert's law in the exponential format as in Equation 1 (Khattari and Al-Buriahi 2022).

$$\frac{I}{I_0} = e^{-\mu t} \quad (1)$$

I_0 is the initial intensity of photons before the attenuation, I is the intensity after the attenuation, t is the thickness of the sample, and the linear attenuation coefficient is shown with μ symbol.

The mass attenuation coefficient (MAC) describes the interaction possibility between gamma photons and a particular medium, and is estimated by the formula as in Equation 2 (Khattari and Al-Buriahi 2022);

$$MAC = \mu_m = \frac{\mu}{\rho} = \frac{1}{\rho t}\ln\left(\frac{I}{I_0}\right) \quad (2)$$

In other words, the photon mass attenuation coefficient is calculated as follows Equation 3;
(Jackson and Hawkes 1981);

$$\frac{\mu}{\rho} = \sum_i w_i \frac{\mu}{\rho_i} \quad (3)$$

where μ/ρ_i is the mass attenuation coefficient of the i^{th} element present in the medium or material and w_i weight fraction.

The thickness of any given material that reduces 50% of the incident energy has been attenuated is defined as the half value layer (HVL). The ten value layer (TVL) parameter is the required thickness which reduces the radiation intensity by one-tenth. The formulas of HVL and TVL are given respectively, in Equations 4 and 5 (Ozpolat *et al*. 2020);

$$HVL = \frac{\ln(2)}{\mu} = \frac{0.693}{\mu} \quad (4)$$

$$TVL = \frac{\ln(10)}{\mu} = \frac{2.302}{\mu} \quad (5)$$

The average distance between two interactions on a photon's way through the material is known as the mean free path (MFP). The MFP may be determined using the following formula (Ozpolat *et al*. 2020);

$$MFP = \frac{1}{\mu} \quad (6)$$

Z_{eff} is the effective atomic number of the material (Ozpolat *et al*, 2020);

$$Z_{eff} = \frac{\sigma_a}{\sigma_e} \quad (7)$$

In this formula, σ_a is the total atomic cross-sections (in unit cm/g), and σ_e is the total electronic cross-sections (cm/g).

N_{eff} explains the electron density-number of electrons per unit mass and is defined as in Equation 8 (Ozpolat *et al*, 2020);

$$N_{eff} = \frac{Z_{eff} N_A}{M} \sum_i n_i \quad (8)$$

Here, M = $\Sigma_i A_i n_i$ is the molecular weight of the compound, and N_A is the Avogadro constant.

The technical details about the shielding-attenuation parameters investigated in this research can be obtained from different research (Ekinci *et al*. 2021, Elazaka *et al*. 2021, Issa 2016, Sing *et al*. 2015).

2.3 Investigated glass samples

In this study, six different samples were used density changed from 3.513 g/cm^3 to 3.643 g/cm^3 for the calculation of radiation parameters via Phy-X/PSD code (Lakshminarayana *et al*, 2023). These samples contain different amounts of elements B (boron), K (potassium), Li (lithium), Te (tellurium), Zn (zinc), Pb (lead), Na (sodium), O (oxygen), F (fluorine) and Er (erbium). The densities and elemental mass fraction (wt. %) of glass samples are indicated in Table 1. The nominal chemical composition of the evaluated glass matrixes are shared in Table 2.

3. Results and Discussions

Evaluating the shielding capabilities of the B_2O_3-TeO_2-ZnO-PbF_2-Er_2O_3 glass matrix by utilizing the Phy-X/PSD program was aimed in this paper. The gamma attenuation parameters of the selected glass group were simulated at different photon energies (0.015 MeV- 15 MeV). Radiation properties of B_2O_3-TeO_2-ZnO-PbF_2-Er_2O_3 glass matrix including Li_2O (E1), Na_2O (E2), K_2O (E3), LiF (E4), NaF (E5), and KF (E6) separately were evaluated. Photons gain energy according to the interaction between the incoming photons and the atomic orbit. In this case, either the photon is completely absorbed or it transfers some of its energy and continues on its way (Tekin et al. 2022). The results show that replacing Li_2O, Na_2O, K_2O, NaF, or KF with LiF causes an increase in the densities of the main glass matrix. On the other hand, it is observed that an increase in the linear attenuation coefficient values. Additionally, the mass attenuation parameter values for B_2O_3-TeO_2-ZnO-PbF_2-Er_2O_3 glasses increase with LiF content. The half-value layers and tenth-value layers had a decreased trend. The fluctuation in the linear attenuation coefficient (LAC) values of the selected six different glass samples is given as a function of photon energy in Figure 1.

Table 1. Elemental mass fraction (wt.%) and densities of samples (Lakshminarayana *et al*. 2023)

Sample Codes	B	Pb	Te	Zn	Er	Li	Na	K	O	F	Density (g/cm^3)
E1	13.2187	21.4700	13.2220	6.7746	3.4662	1.4384	0	0	36.4727	3.9372	3.513
E2	12.7932	20.7789	12.7963	6.5565	3.3546	0	0.4610	0	35.2987	3.8105	3.560
E3	12.3929	20.1286	12.3958	6.3514	3.2497	0	0	7.5963	34.1940	3.6912	3.576
E4	13.2729	21.5581	13.2761	6.8024	3.4804	0.7222	0	0	34.9577	5.9300	3.643
E5	13.0550	21.2040	13.0581	6.6907	3.4233	0	2.3527	0	34.3835	5.8326	3.598
E6	12.8432	20.8601	12.8463	6.5822	3.3678	0	0	3.9362	33.8259	5.7381	3.559

Table 2. Nominal chemical composition of the synthesized glasses (mol%) (Lakshminarayana *et al*. 2023)

Sample Codes	B_2O_3	PbF_2	TeO_2	ZnO	Er_2O_3	Li_2O	Na_2O	K_2O	LiF	NaF	KF
E1	59.0	10	10	10	1.0	10	0	0	0	0	0
E2	59.0	10	10	10	1.0	0	10	0	0	0	0
E3	59.0	10	10	10	1.0	0	0	10	0	0	0
E4	59.0	10	10	10	1.0	0	0	0	10	0	0
E5	59.0	10	10	10	1.0	0	0	0	0	10	0
E6	59.0	10	10	10	1.0	0	0	0	0	0	10

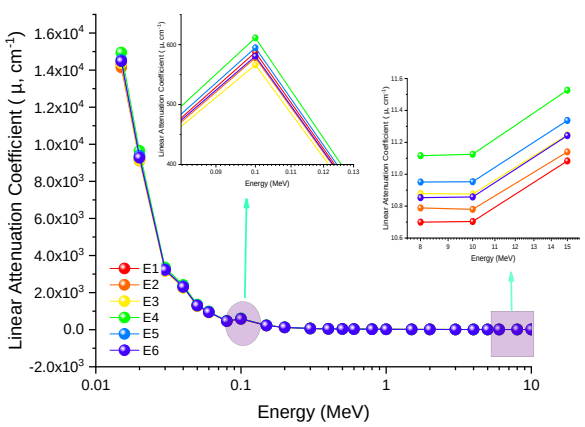

Figure 1. Variations of linear attenuation coefficients with respect to photon energy for E1-E6 glasses.

When radiation is penetrated into matter, various interaction events occur. When gamma rays or x-rays are directed into a material, a number of the photons interact with the particles of the matter/medium and after that photon energies can be scattered or absorbed. This scattering or absorption phenomenon is defined as attenuation. Therefore, attenuation parameters are affected by different types of interactions. Based on Figure 1, the trend in the linear attenuation coefficient curves is suited to Beer–Lambert law. The linear attenuation coefficient decreased smoothly at high energies, but at lower energies, the LAC decreased greatly.

The Z_{eff} values of glass samples are given in Figure 2. The findings show that the Z_{eff} softly increased with the LiF and NaF. The Z_{eff} depends on the constituent elements of the sample and the energy. The photon numbers transmitted through a material depend upon the energy of the individual photons and atomic number, the density, and the thickness of the material. For this reason, Z_{eff} is a critical quantity in shielding studies. The highest effective atomic number values were obtained at low energies among the samples' 0.015 MeV and 0.1 MeV energies. The E4 and E5 samples have higher values at ~0.1 MeV than others. The behavior of Z_{eff} with the energy can be ascribed with the Compton scattering (explains the constancy in Z_{eff}), the photoelectric effect (related to the quick decreasing in Z_{eff}), and pair production (Al-Hadeethi and Sayyed 2020b).

The mass attenuation coefficient values of glass structures are demonstrated in Figure 3. For the mass attenuation coefficient, the maximum value was acquired in the E4 sample containing lithium fluoride (LiF) at 0.015 MeV. The value layer parameters (HVL and TVL) are significant penetrating quantity parameters. They are used to define the thickness of the absorber that is required to block half or 90% of the initial intensity. Fluctuations of half value layer quantity for all E1-E6 sample glasses are shown in Figure 4.

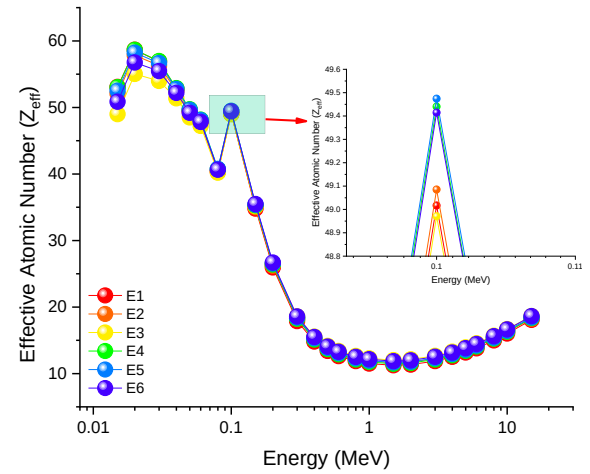

Figure 2. The effective atomic number of selected glass samples

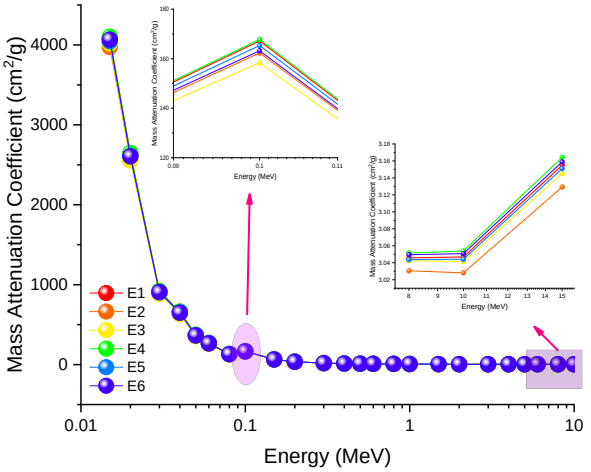

Figure 3. Variations of mass attenuation coefficients (cm^2/g) with respect to photon energy for selected E1-E6 glasses

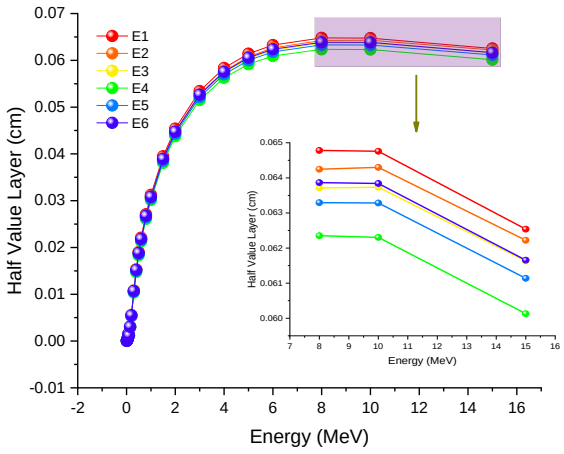

Figure 4. Variations of HVL (cm) with photon energy for E1-E6 sample glasses

The HVL and TVL quantities depend actually on the energy of the photon and the density of the material. The HVL is described as the thickness of an absorber or a shield that is required to block the intensity of the gamma rays by a factor of one-half. In Figure 4, HVL values vary between 0.000 and 0.065 cm. According to the data of this study, sample E4 has the lowest half-value layer but the highest density and linear attenuation coefficients. As seen in Figure 4, in the high energy region, that is, at 15 MeV, sample E1 has the highest HVL value, while sample E4 has the lowest HVL value. As the amount of penetration of a photon stream into the matter increases, more HVL thickness is required or such material should be chosen so that the same effect can be achieved at smaller HVL values.

The tenth value layer for the B_2O_3-TeO_2-ZnO-PbF_2- Er_2O_3 is also presented, and the effect of different compositions such as Li_2O, Na_2O, K_2O, LiF, KF, and NaF were investigated. The relation between the tenth layer value and the energy for the samples is presented in Figure 5. The tenth value layer gradually increased as the energy changed from 0.015 to 15 MeV. The TVL takes the order of E1> E2> E6> E3> E5> E4> at all energies. The TVL curves showed that adding LiF to the main glass structure in the synthesized glass form can reduce the needed thickness amount for the block to photons.

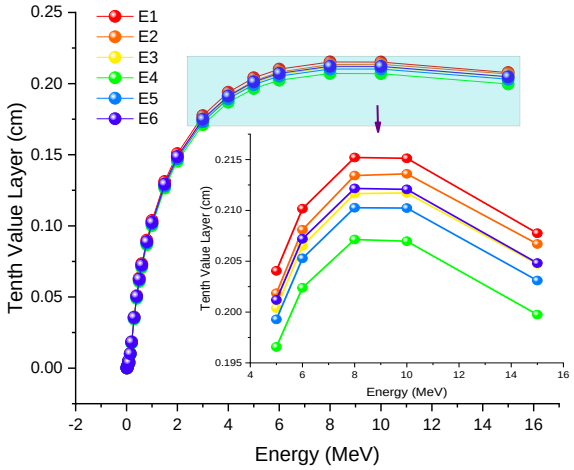

Figure 5. Variations of TVL (cm) with photon energy for E1-E6 sample glasses

The mean free path (MFP) for the selected glasses was performed by the Phy-X/PSD codes and the outputs were plotted as a function of the energy. Fluctuations of mean free path values for E1-E6 glasses are given in Figure 6.
The average distance traveled by a photon between collisions is known mean free path. MFP is abied by the density of the material. Mostly, when the density of samples increases, the mean free path gradually decreases. Additionally, with increasing material density, the attenuation properties become better. The mean free path values varied within the range of 0-0.087 cm for the E4 sample. As a result, the addition of suitable heavy

metal oxides with appropriate ratios to the chosen glass directly impacts the density of the glass.

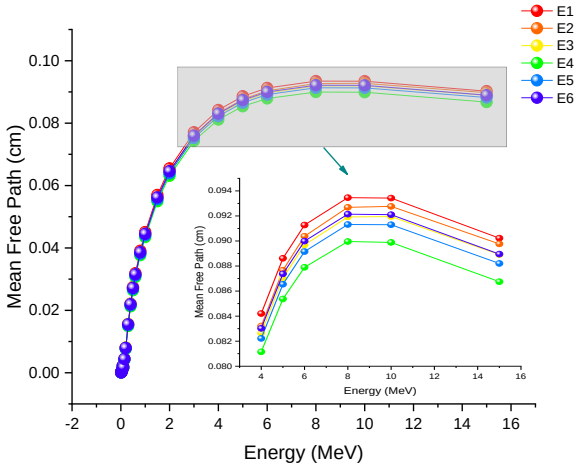

Figure 6. Variations of mean free path values as a function of photon energy for E1-E6 sample glasses

The effective electron density (N_{eff}) graph is given in Figure 7. Glass sample encoded with E1 reaches maximum effective electron density in the high energy region.

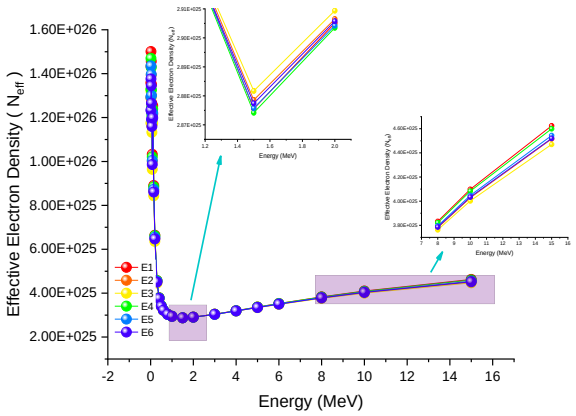

Figure 7. Variations of effective electron density as a function of photon energy for E1-E6 sample glasses

4. Conclusions

In this comprehensive investigation into the radiation attenuation properties of B_2O_3-TeO_2-ZnO-PbF_2-Er_2O_3 glass systems doped with various alkali metal oxides and fluorides (Li_2O, Na_2O, K_2O, LiF, NaF, KF), several critical insights have been observed. The study distinctly showcases how the integration of different alkali elements in the glass matrix impacts its radiation shielding capabilities. A notable increase in the linear attenuation coefficient and a corresponding decrease in half-value and tenth-value layers, particularly when LiF was substituted for Li_2O, Na_2O, and K_2O. This suggests that the presence of LiF significantly enhances the glass's density and its ability to attenuate radiation. This finding is particularly relevant for the development of high-density glass materials for radiation shielding applications. The slight increase in the effective atomic number (Z_{eff}) and effective electron density (N_{eff}) with the addition of Li_2O/LiF combination is another key finding. The synergy between Li_2O and the heavy metal PbF_2 in this glass matrix presents a promising avenue for creating effective radiation shielding materials. These glasses offer a balance between density, transparency, and shielding effectiveness, making them suitable for various applications where both visibility and radiation protection are required, such as in medical imaging or nuclear facilities. Looking forward, this research opens up several avenues for further exploration. Future studies could delve into the long-term stability and durability of these glass systems under radiation exposure, which is critical for their practical application. Additionally, investigating the thermal properties and chemical resistance of these glasses can provide a more comprehensive understanding of their suitability in different environmental conditions. Exploring the potential of other dopants or combinations thereof could also lead to the discovery of glass compositions with even superior shielding properties.

Moreover, the scalability and economic viability of manufacturing these glass types on a larger scale is an area that warrants further investigation, especially considering their potential application in industrial and medical settings. In conclusion, the study has not only expanded the understanding of the radiation shielding capabilities of B_2O_3-TeO_2-ZnO-PbF_2-Er_2O_3 glass systems but also highlighted the significant role of alkali metal oxides and fluorides in enhancing these properties. The promising results obtained with LiF, in particular, suggest a potential pathway for developing more effective and efficient radiation shielding materials in the future.

Declaration of Ethical Standards

The authors declare that they comply with all ethical standards.

Credit Authorship Contribution Statement

Author-1: Conceptualization, investigation, methodology and software, visualization and writing, supervision, review and editing – original draft.

Declaration of Competing Interest

The author has no conflicts of interest to declare regarding the content of this article.

Data Availability Statement

All data generated or analyzed during this study are included in this published article.

5. References

Abou Hussein, E. M., et al., 2021. Gamma ray interaction of optical, chemical, physical behavior of bismuth silicate glasses and their radiation shielding proficiency using Phy-X/PSD program. *Journal of Non-Crystalline Solids*, **570**, 121021.

https://doi.org/10.1016/j.jnoncrysol.2021.121021

Agar, O., et al., 2019. Evaluation of the shielding parameters of alkaline earth based phosphate glasses using MCNPX code, *Results Phys*, **12,** 101. https://doi.org/10.1016/j.rinp.2018.11.054

Akkurt, I., and Malidarre, R. B., 2022. Physical, structural, and mechanical properties of the concrete by FLUKA code and phy-X/PSD software. *Radiation Physics and Chemistry*, **193**, 109958. https://doi.org/10.1016/j.radphyschem.2021.109958

Alan, H. Y., et al., 2023. Non-decreasing monotonic effects of cerium and gadolinium on tellurite glasses toward enhanced heavy-charged particle stopping: alpha-proton particles as major a part of cosmic radiation. *Journal of the Australian Ceramic Society*, 1-10. https://doi.org/10.1007/s41779-023-00984-7

Al-Buriahi, M. S., et al. 2021. Newly developed glasses containing Si/Cd/Li/Gd and their high performance for radiation applications: role of Er 2 O 3. *Journal of Materials Science: Materials in Electronics*, **32**, 9440-9451. https://doi.org/10.1007/s10854-021-05608-z

Al-Hadeethi, Y., and Sayyed, M. I., 2020a. A comprehensive study on the effect of TeO2 on the radiation shielding properties of TeO2–B2O3–Bi2O3–LiF–SrCl2 glass system using Phy-X/PSD software. *Ceramics Internationa*l, **46(5)**, 6136-6140. https://doi.org/10.1016/j.ceramint.2019.11.078

Al-Hadeethi, Y., and Sayyed, M. I., 2020b. Evaluation of gamma ray shielding characteristics of CaF2–BaO–P2O5 glass system using Phy-X/PSD computer program. *Progress in Nuclear Energy*, **126**, 103397. https://doi.org/10.1016/j.pnucene.2020.103397

ALMisned, G. et al. 2023. Bismuth (III) oxide and boron (III) oxide substitution in bismuth-boro-zinc glasses: A focusing in nuclear radiation shielding properties. *Optik*, **272**, 170214. https://doi.org/10.1016/j.ijleo.2022.170214

Almuqrin, A. H., et al., 2021. Li2O-K2O-B2O3-PbO glass system: Optical and gamma-ray shielding investigations. *Optik*, **247**, 167792. https://doi.org/10.1016/j.ijleo.2021.167792

Arpaci, N., and Aygun, M. 2022. Determınatıon Of Radıatıon Shıeldıng Parameters Of Cocrfenıtıalx Alloys By Usıng Recently Developed Phy-X/Psd And Epıxs Softwares. *Journal Of Amasya University The Institute Of Sciences And Technology*, **3(1)**, 8-22. https://doi.org/10.54559/jauist.1075966

Aygun Z., and Aygun M., 2023. Evaluation of radiation shielding potentials of Ni-based alloys, Inconel-617 and Incoloy-800HT, candidates for high temperature applications especially for nuclear reactors, by EpiXS and Phy-X/PSD codes, *Journal of Polytehnic*, **26(2)**, 795-801. https://doi.org/10.2339/politeknik.1004657

Deliormanli, A. M., et al. 2021. Erbium (III)-and Terbium (III)-containing silicate-based bioactive glass powders: physical, structural and nuclear radiation shielding characteristics. *Applied Physics A*, **127(6),** 463. https://doi.org/10.1007/s00339-021-04615-5

Effendy, N., et al., 2021. Influence of ZnO to the physical, elastic and gamma radiation shielding properties of the tellurite glass system using MCNP-5 simulation code. *Radiation Physics and Chemistry*, **188**, 109665. https://doi.org/10.1016/j.radphyschem.2021.109665

Ekinci, N., et al., 2014. A study of the energy absorption and exposure buildup factors of some anti-inflammatory drugs, *Appl. Radiat. Isot*. **90**, 265–273. https://doi.org/10.1016/j.apradiso.2014.05.003

Elazaka, A.L., et al., 2021. New approach to removal of hazardous Bypass Cement Dust (BCD) from the environment: 20Na2O–20BaCl2-(60-x)B2O3-(x)BCD glass system and optical, mechanical, structural and nuclear radiation shielding competences, *J. Hazard. Mater*. **403**, 123738. https://doi.org/10.1016/j.jhazmat.2020.123738

El-Denglawey, A., et al., 2021. The impact of PbF2-based glasses on radiation shielding and mechanical concepts: an extensive theoretical and Monte Carlo simulation study. *Journal of Inorganic and Organometallic Polymers and Materials*, **31(10)**, 3934-3942. https://doi.org/10.1007/s10904-021-02088-w

Issa, Shams S.A., 2016. Effective atomic number and mass attenuation coefficient of PbO–BaO–B2O3 glass system. *Radiation Physics and Chemistry*. **120**,33–37. https://doi.org/10.1016/j.radphyschem.2015.11.025

Jackson, D.F., and Hawkes, D.J., 1981. X-ray attenuation coefficients of elements and mixtures. *Physics Report* **70**, 169–233. https://doi.org/10.1016/0370-1573(81)90014-4

Karpuz, N., 2023. Radiation shielding properties of glass composition. *Journal of Radiation Research and Applied Sciences*, **16(4),** 100689. https://doi.org/10.1016/j.jrras.2023.100689

Katubi, K. M., et al. 2022. Enhancement on radiation shielding performance of B2O3+ Li2O+ ZnO+ Na2O glass system. *Radiation Physics and Chemistry,* **201**, 110457. https://doi.org/10.1016/j.radphyschem.2022.110457

Khattari, Z. Y., and Al-Buriahi, M. S., 2022. Monte Carlo simulations and Phy-X/PSD study of radiation shielding effectiveness and elastic properties of barium zinc aluminoborosilicate glasses. *Radiation Physics and Chemistry*, **195**, 110091. https://doi.org/10.1016/j.radphyschem.2022.110091

Lakshminarayana, G., et al. 2017. Structural, thermal and optical investigations of Dy3+-doped B2O3–WO3–ZnO–Li2O–Na2O glasses for warm white light emitting applications, *J. Lumin*. **186**,

https://doi.org/10.1016/j.jlumin.2017.02.049

Lakshminarayana, G., et al., 2023. Er3+: B2O3-TeO2-ZnO-PbF2− M2O/MF (M= Li, Na, and K) glasses: An inspection of structural, thermal, optical, chromatic, and near-infrared luminescence traits for displays and potential C-band amplification. *Journal of Non-Crystalline Solids*, **622**, 122660. https://doi.org/10.1016/j.jnoncrysol.2023.122660

Malidarre, R. B., et al., 2021. Fast neutrons shielding properties for HAP-Fe2O3 composite materials. *International Journal of Computational and Experimental Science and Engineering*, **7(3),** 143-145. https://doi.org/10.22399/ijcesen.1012039

Metwalli, E., et al. 2004. Properties and structure of copper ultraphosphate glasses, *J. Non-Cryst. Solids*, **344**, (2004) 128. https://doi.org/10.1016/j.jnoncrysol.2004.07.058

Mokhtari, K., et al., 2021. Fabrication, characterization, simulation and experimental studies of the ordinary concrete reinforced with micro and nano lead oxide particles against gamma radiation. *Nuclear Engineering and Technology*, **53(9),** 3051-3057. https://doi.org/10.1016/j.net.2021.04.001

Oruncak, B., 2023. Radiation shielding properties for 90 (Se)-(10-x)(Te)-x (Ag) chalcogenide glasses. *Journal of Radiation Research and Applied Sciences,* **16(4),** 100723. https://doi.org/10.1016/j.jrras.2023.100723

Ozpolat, Ö. F., et al., 2020. Phy-X/ZeXTRa: a software for robust calculation of effective atomic numbers for photon, electron, proton, alpha particle, and carbon ion interactions. *Radiation and Environmental Biophysics*, **59(2),** https://doi.org/10.1007/s00411-019-00829-7

Rammah, Y. S., et al. 2020. Role of ZnO on TeO2. Li2O. ZnO glasses for optical and nuclear radiation shielding applications utilizing MCNP5 simulations and WINXCOM program. *Journal of Non-Crystalline Solids*, **544**, 120162. https://doi.org/10.1016/j.jnoncrysol.2020.120162

Rammah, Y. S., et al., 2021. The impact of PbF2 on the ionizing radiation shielding competence and mechanical properties of TeO2–PbF2 glasses and glass-ceramics. *Ceramics International*, **47(2),** 2547-2556. https://doi.org/10.1016/j.ceramint.2020.09.100

Şakar, E., et al., 2020. Phy-X/PSD: development of a user friendly online software for calculation of parameters relevant to radiation shielding and dosimetry. *Radiation Physics and Chemistry*, **166**, 108496. https://doi.org/10.1016/j.radphyschem.2019.108496

Sayyed, M. I., 2023. The impact of Chemical composition, density and thickness on the Radiation Shielding properties of CaO–Al2O3–SiO2 glasses. *Silicon*, 1-10. https://doi.org/10.1007/s12633-023-02640-y

Singh, V. P., Badiger, N. M., and Kaewkhao, J., 2014. Radiation shielding competence of silicate and borate heavy metal oxide glasses: comparative study. *Journal of non-crystalline solids*, **404**, 167-173. https://doi.org/10.1016/j.jnoncrysol.2014.08.003

Singh, G., et al, 2015. Measurement ofattenuation coefficient, effective atomic number and electron density of oxides of lanthanides by using simplified ATM-method. *J. Alloy. Compd.* **619**, 356–360. https://doi.org/10.1016/j.jallcom.2014.09.026

Susoy, G., 2020. Effect of TeO2 additions on nuclear radiation shielding behavior of Li2O–B2O3–P2O5–TeO2 glass-system. *Ceramics International*, **46(3),** 3844-3854. https://doi.org/10.1016/j.ceramint.2019.10.108

Şengül, A., 2023. Gamma-ray attenuation properties of polymer biomaterials: Experiment, XCOM and GAMOS results. *Journal of Radiation Research and Applied Sciences,* **16(4),** 100702. https://doi.org/10.1016/j.jrras.2023.100702

Tekin, H.O., et al., 2019. An extensive investigation on gamma-ray and neutron attenuation parameters of cobalt oxide and nickel oxide sub-stituted bioactive glasses, *Ceram. Int*. **45 (8),** 9934–9949. https://doi.org/10.1016/j.ceramint.2019.02.036

Tekin, H. O., et al., 2022. Transmission factor (TF) behavior of Bi2O3–TeO2–Na2O–TiO2–ZnO glass system: a Monte Carlo simulation study. *Sustainability*, **14(5),** 2893. https://doi.org/10.3390/su14052893

Zaid, M. H. M., et al., 2012. Effect of ZnO on the physical properties and optical band gap of soda lime silicate glass. *International journal of molecular sciences,* **13(6)**, 7550-7558. https://doi.org/10.3390/ijms13067550

Yilmaz, A., et al., 2023. Exploring the KERMA, mass stopping power and projected range values against heavy-charged particles: A focusing study on Sm, Yb, and Nd reinforced tellurite glass shields. *Radiation Physics and Chemistry*, **212**, 111167. https://doi.org/10.1016/j.radphyschem.2023.111167

Yılmaz, D., et al. 2020. Erbium oxide and Cerium oxide-doped borosilicate glasses as radiation shielding material. *Radiation Effects and Defects in Solids*, **175(5-6),** 458-471. https://doi.org/10.1080/10420150.2019.1674301

Internet References

1-https://phy-x.net/module/physics/shielding/ (02.04.2023)